Derivation of a simple engineering equation for the minimum voltage of inverted fireball onset

J. Gruenwald[1]

[1]Gruenwald Laboratories GmbH, Taxberg 50, 5660 Taxenbach, Austria

(Received: 09. November 2022, Accepted: 23. November 2022, Published online: 23. November 2022)

This paper describes the derivation of a simple engineering equation to calculate the minimal necessary bias voltage for the onset of an inverted fireball. The calculation uses the electron density in the absence of an inverted fireball as well as the grid constant and the working gas species as input parameters. It will be shown that the interplay between ionsation potential, dissociation potential (for molecular working gases), as well as the electron density in the background plasma, play an important role in the necessary minimum bias on the fireball electrode. Some of the most common working gases and their relevant parameters will also be listed in this paper. This should give experimentalists and engineers a practical equation that can be used to quickly determine the most important electrical properties of the anode that is used to trap the inverted fireball. Thus, the planning and design of experimental setups or technological devices will be made much less time-consuming and, thus, more convenient.

DOI: 10.31281/jtsp.v3i1.26

jgruenwald@gmx.at

I. Introduction

Inverted fireballs (IFBs) have been discovered in 2011 [1, 2]. In those early works, IFBs were the subject of pure experimental research that was dedicated to studying non-linearities and instabilities inside highly transparent, grid electrodes. Over the last 15 years, IFBs have drawn increased attention due to their possible technological applications. For example, they can be used to convert dc voltage signals directly into rf signals [2]. However, the strongest research focus has been put on their usage in surface treatment technologies, especially in the field of carbon coatings [3, 4, 5] or sputtering [6]. It has also been demonstrated recently that the plasma parameter inside and IFB can be controlled to a certain extent by segmented biasing of the IFB anode [7]. There have also been attempts to integrate an IFB setup into a magnetron sputter chamber but with inconclusive results [8], which show that there is still a lot of work to be done to get a good understanding of this phenomenon. However, some basic principles of IFBs are well understood. They essentially form a Faraday cage due to the electric closure of the hollow grid anode. Thus, the plasma potential on the inside assumes a constant value. This leads to a very homogeneous plasma. On the other hand, electrons from the surrounding background plasma are injected into the IFB with high kinetic energy. These energetic electrons either ionise a neutral particle in the IFB or pass right through it. In the latter case, they immediately feel the electric field as soon as they leave the IFB and are pulled back into it. This oscillating behavior not only leads to transit time instabilities but also enhances the plasma density within the IFB. Additionally, a potential well is formed due to a potential overshoot near the inner edge of the grid electrode, similar to the one described by Ecker [9]. This potential well traps the relatively cold ions and, hence, creates a chemically very reactive plasma. This favorable combination of homogeneous plasma potential and elevated density makes them an ideal tool for surface modification, especially deposition. To make IFBs a really viable deposition tool, they have to be controlled and monitored. This is often a tedious task because of the large parameter space that has to be covered when setting up the experiment or coating chamber. The combination with the somehow incomplete understanding of basic physics involved in IFBs very often leads to time-consuming trial-and-error test runs for finding the optimal parameter set. This paper tries to solve this problem to some extent by deriving a simple formula for the minimum voltage required for IFB ignition. The free parameters are the electron density in absence of the IFB (i.e. the background plasma density), the grid constant of the IFB anode, the mass, and the ionisation (or dissociation) potential of the working gas. This reduces the parameter space a great deal and simplifies the design of IFB setups.

II. The Practical Equation

IFBs need equipotential closure to be formed. This was demonstrated in Ref. [10] and is depicted in the following Fig. 1. Thus, the grid constant d and the Debye length have to obey the relation: $\lambda_D \geq d/2$.

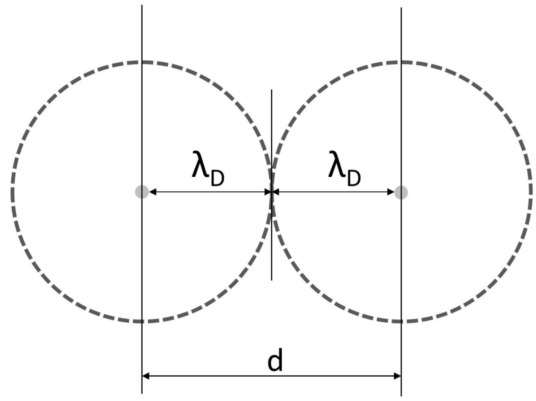

Figure 1: Schematics for the condition of equipotential surface closure around an IFB.

It is evident from Fig. 1 that the Debye sheaths of two neighboring grid wires have to touch each other in order the close the equipotential surface. For the derivation of the IFB bias voltage, the electron Debye length can be used. It is given by:

$$\lambda_D = \sqrt{\frac{\epsilon_0 k T_e}{n_e e^2}} \tag{1}$$

Here ϵ_0 denotes the permittivity of free space, k is Boltzmann's constant, T_e is the electron temperature in eV, e is the elementary charge and n_e denotes the plasma density in absence of an IFB. Since the potential drop in the sheath surrounding the gridded anode is usually in the order of the first ionisation potential ϕ_{ion} [11, 12, 7], the potential on the IFB electrode (in Volt) is given by:

$$\phi_{IFB} \approx \phi_{pl} + \phi_{ion} + \phi_{diss} \tag{2}$$

The term ϕ_{diss} describes the dissociation energy, which only comes into play for molecular gases and only if the dissociation energy is below the first ionisation potential. This is the usual case for most of the common working gases. Two measured examples of this potential jump in an IFB double layer, namely in molecular hydrogen and helium, are depicted in the following Fig. 2:

Since the dissociation potential has to be supplied by the electric field of the IFB electrode along with the ionisation energy, it has to be added to Eq. (2) if needed. The potential drop on the edge of the hydrogen IFB was measured with 18.2 V in Fig. 2. The dissociation energy of the hydrogen bond is 4.4 eV, while the first ionisation potential of atomic hydrogen is 13.6 eV. This sums up to 18 eV, which is in perfect agreement with the presented data. Helium, on the other hand, has its first ionisation energy at 24 eV. Thus, the data for He in Fig. 2 is less accurate but still lies within the typical error bars of a Langmuir probe (10 - 15 %).

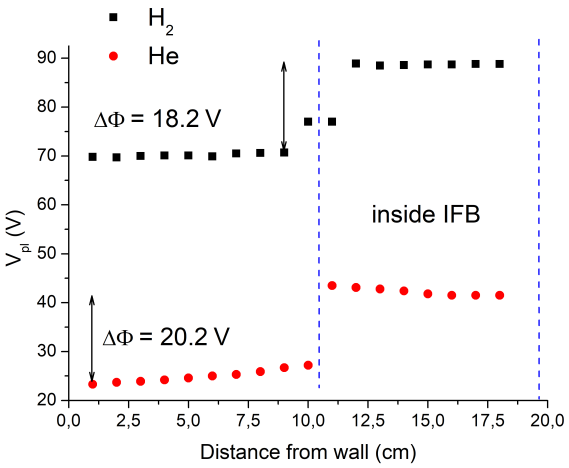

Figure 2: Langmuir probe measurements of the plasma potential from two different experiments. Experimental parameters: H_2 - 7 x 10^{-3} mbar, U_{IFB} +100 V vs. ground. He - p = 1.5 x 10^{-1} mbar, U_{IFB} +75 V vs. ground

Furthermore, the plasma potential in a quasi-neutral plasma with Maxwellian electron energy distribution is connected to the electron temperature via [13, 14]:

$$\phi_{pl} = \frac{T_e}{2} \cdot \left[1 + ln\left(\frac{2M_i}{\pi m_e}\right)\right], \tag{3}$$

where M_i is the mass of the working gas ion and m_e denotes the electron mass. Solving Eq. (3) for T_e and using the expression for the plasma potential from Eq. 2, one obtains:

$$T_e = \frac{2 \cdot (\phi_{IFB} - \phi_{ion} - \phi_{diss})}{\left[1 + ln\left(\frac{2M_i}{\pi m_e}\right)\right]} \tag{4}$$

Plugging this expression for T_e into the formula for the Debye length and combining it with the inequality for the requirement of minimal grid distance d yields:

$$\frac{d}{2} \leq \sqrt{\frac{\epsilon_0}{n_e e}} \cdot \sqrt{\frac{2 \cdot (\phi_{IFB} - \phi_{ion} - \phi_{diss})}{\left[1 + ln\left(\frac{2M_i}{\pi m_e}\right)\right]}} \tag{5}$$

It has to be noted that Eq. 4 gives the electron temperature in eV. However, for further calculations, SI units are used to keep things simple. Hence, the factor $\frac{k_B}{e}$ is neglected in the expression for the Debye length from now on. This converts the value for the electron temperature directly into K. Solving Eq. (5) for the potential on the IFB grid electrode and summarising all the natural constants with the abbreviation K yields in SI units:

$$\begin{aligned} \phi_{FB} \geq (\phi_{ion} + \phi_{diss}) + \frac{d^2}{8} \cdot K \cdot \\ \cdot n_e \cdot \left[1 + ln\left(\frac{2M_i}{\pi m_e}\right)\right] \end{aligned} \tag{6}$$

Here K is a constant with the value of $1.8 \cdot 10^{-8}$ V/m. A list of the parameters of some common working gases is shown in Tab. 1:

For example, a low-pressure helium plasma with a background density (i. e. the plasma density in absence of an IFB) of $5 \times 10^{15} m^{-3}$ and an IFB electrode grid constant of 200 microns would require $\phi_{IFB} \geq 24.6eV + 4 \times 10^{-8}/8 \times 1.8 \times 10^{-8} V/m \times 5 \times 10^{15} m^{-3} \times (1 + ln(4513)) = 28.8 \approx$ 30 V for igniting the IFB. It has to be emphasized at this point that this is the absolute minimum voltage requirement for keeping the IFB burning.

The following Fig. 3 shows different minimum voltages for IFB onset as a function of the grid wire distance for a background plasma density of $10^{15} m-3$. It can readily be seen that the onset voltage scales with the square of d, in accordance with Eq. (6). However, the largest influence stems from the ionisation and dissociation potential of the working gas.

Another important quantity for IFB ignition is the background plasma density. As shown in Fig. 4, increasing the background plasma density leads to larger bias requirements for the IFB electrode. This is because in order to establish full electric closure around the mesh, the Debye length has to be large enough. Higher electron densities decrease λ_D, which needs to be compensated by a higher average electron temperature. The electron temperature, on the other hand, can partially be influenced by stronger electric fields on the IFB anode. Therefore, the minimum ignition voltage has to increase with higher background plasma density.

It has to be emphasized at this point that the approach in this paper is an abridged one that only holds for noble gases and simple molecules. The reason is that more complex working gas species have higher masses (HMDSO, for example, has about 252×10^{-27} kg - an order of magnitude more than methane). This leads to higher minimum bias voltages on the grid electrode, especially when the background plasma is very dense as well. However, higher IFB voltage leads to electrons with a higher kinetic energy that, in turn, shatter complex molecules even further. If the initial working gas molecule becomes more fragmented, the mass of the ions is reduced. Thus, there can be a much more complex interplay between the bias requirement, the mass of the ions, and the background plasma density. In such cases, the complexity of the IFB plasma system increases drastically and it is not possible to find a simple analytic expression for the IFB onset voltage. It might be possible to derive an equation, which is analytically solvable but it will be a very complicated one. This is beyond the scope of this paper, which aims at providing a simple yet applicable formula for calculating the voltage requirements for IFB experiments. Eq. (6) represents an equation that can be used for an already wide range of simple working gases. Most of them are frequently used in fundamental physics experiments but also in technological applications, such as PECVD, plasma etching, or other types of plasma surface modifications. Table 1 lists all the necessary parameters that are needed to calculate the onset voltage for some of the most commonly relevant process gases.

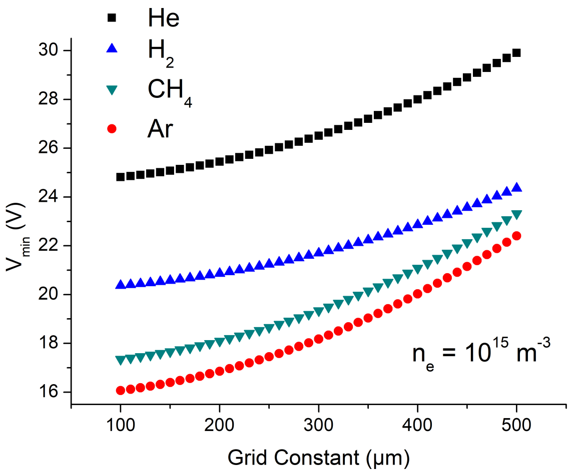

Figure 3: The required minimum bias voltage (vs. ground) for IFBs in helium, hydrogen, methane and argon as a function of the grid spacing. The plasma density was assumed to be constant at $n_e = 10^{15} m^{-3}$

III. Summary and Outlook

In this paper a simple equation was derived that predicts the minimal onset voltage of IFBs. It is only based on a handful of easy-to-obtain parameters, some of them just material constants. Example calculations for realistic experimental con-

Gas species	M_i **[10^{-27}kg]**	ϕ_{ion} **[eV] - for atoms [15]**	ϕ_{diss} **[eV]**
Helium	6.6	24.6	
Neon	33.4	21.6	
Argon	66.4	15.8	
Krypton	139.2	14.0	
Xenon	218.0	12.1	
Radon	368.6	10.7	
H_2	0.85 (for the H atom)	13.6	4.4 [15]
N_2	11.6 (for the N atom)	14.5	9.8 [15]
O_2	13.3 (for the O atom)	13.6	5.1 [15]
CO	20.0 (for the C atom)	14.0	11.6 [15]
CO_2	33.3 (for CO)	13.8	5.5 for separating 1 O [16]
CH_4	24.3 (for CH_3)	12.6	4.5 for separating 1 H [17]

Table 1: Relevant physical parameters for the most important working gases. Note that the mass of the ions is given for the (partly) dissociated molecules.

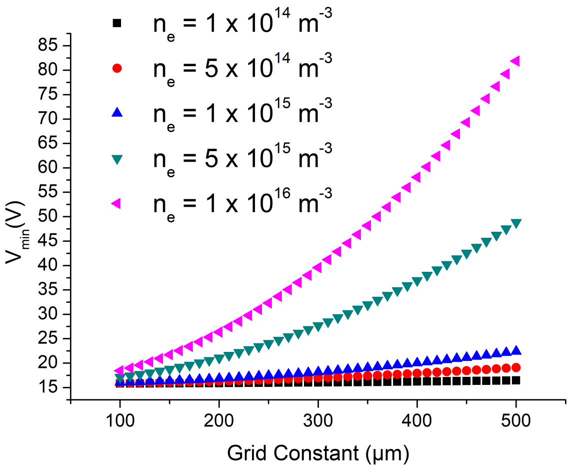

Figure 4: The required minimum bias voltage (vs. ground) for argon in different background plasma densities as a function of the grid constant.

ditions have been performed and the most important parameters for commonly used working gases have been listed for the convenience of the reader. It was shown that the onset bias of an IFB is not only dependent on the grid constant but also on the ion mass and the ionisation and dissociation energy of the working gas particles. It is a very simple approach that provides a fast method to calculate the bias voltage necessary for IFB ignition. As is also pointed out in this paper, some complex process gases, such as HMDSO require a different physical and mathematical treatment due to their potentially complex interplay between bias voltage, ionisation and fragmentation of the working gas molecules. Finding a suitable relationship for more complex gaseous compounds might be possible but is beyond the scope of this work. Thus, this is left for future investigations.

IV. References

[1] R. L. Stenzel, J. Gruenwald, B. Fonda, C. Ionita, and R. Schrittwieser, “Transit time instabilities in an inverted fireball. II. mode jumping and nonlinearities,” *Phys. Plas.*, vol. 18, no. 1, p. 012105, 2011.

[2] R. L. Stenzel, J. Gruenwald, B. Fonda, C. Ionita, and R. Schrittwieser, “Transit time instabilities in an inverted fireball. I. basic properties,” *Phys. Plas.*, vol. 18, no. 1, p. 012104, 2011.

[3] M. Mayer, J. Reynvaan, J. Gruenwald, K. Krenn, T. Schoeberl, S. Surnev, and P. Knoll, “Diamond like carbon deposition by inverted fireballs,” *Materials Today: Proceedings*, vol. 3, pp. S184–S189, 2016.

[4] G. Eichenhofer, M. Oberberg, J. Eisenlohr, P. Awakowicz, and J. Grünwald, “Measurement of inverted n-hexane fireball properties with

a multipole resonance probe," *The Journal of Technological and Space Plasmas*, vol. 3, no. 1, pp. 109–117, 2022.

[5] J. Gruenwald, G. Eichenhofer, G. Filipič, Ž. Federl, W. Feuchtenberger, K. Panos, G. H. Rodríguez, and A. Coclite, "Inverted fireball deposition of carbon films with extremely low surface roughness," *Carbon Letters*, pp. 1–7, 2022.

[6] P. Knoll, J. Reynvaan, M. Mayer, S. Surnev, P. Geistlinger, K. Krenn, K. Ettinger, C. Prietl, A. Hohenau, J. Gruenwald, *et al.*, "Pecvd of carbon by inverted fireballs: From sputtering, bias enhanced nucleation to deposition," *Diamond and Related Materials*, vol. 65, pp. 96–104, 2016.

[7] J. Gruenwald, J. Reynvaan, and P. Geistlinger, "Influence of inhomogeneous electrode biasing on the plasma parameters of inverted H_2 fireballs," *J. Technol. Space Plasmas*, vol. 1, no. 1, pp. 1–4, 2020.

[8] J. Gruenwald, M. Balzer, G. Eichenhofer, and M. Fenker, "Application and limitations of inverted fireballs in a magnetron sputter device," *Surface and Coatings Technology*, vol. 422, p. 127510, 2021.

[9] G. Ecker, "Anode spot instability I. The Homogeneous Short Gap Instability," *IEEE Trans. Plasma Sci.*, vol. 2, no. 3, pp. 130–146, 1974.

[10] J. Gruenwald, R. L. Stenzel, C. Ionita, and R. Schrittwieser, "Further experiments on inverted fireballs," *Conference Proceedings of the 38th EPS Conference on Plasma Physics*, vol. 1, pp. 265–269, 2011.

[11] J. Gruenwald, J. Reynvaan, and P. Knoll, "Creation and characterization of inverted fireballs in H_2 plasma," *Phys. Scr.*, vol. 2014, no. T161, p. 014006, 2014.

[12] J. Gruenwald, J. Reynvaan, and P. Geistlinger, "Basic plasma parameters and physical properties of inverted he fireballs," *Plasma Sources Science and Technology*, vol. 27, p. 015008, jan 2018.

[13] M. A. Lieberman and A. J. Lichtenberg, *Principles of plasma discharges and materials processing*. John Wiley & Sons, 2005.

[14] D. Levko and J. Gruenwald, "Influence of the emission current on a beam-generated plasma," *Physics of Plasmas*, vol. 25, no. 12, p. 123509, 2018.

[15] R. C. Weast, ed., *Handbook of Chemistry and Physics, 86th edition*. CRC Press, 2005.

[16] M. A. Lindon and E. E. Scime, "Co2 dissociation using the versatile atmospheric dielectric barrier discharge experiment (vader)," *Frontiers in Physics*, vol. 2, 2014.

[17] S. J. Blanksby and G. B. Ellison, "Bond dissociation energies of organic molecules," *Accounts of Chemical Research*, vol. 36, no. 4, pp. 255–263, 2003. PMID: 12693923.